A generalized GPR application potential zonation in the karst catchment of SW China

Qiangshan Gao (gaoqiangshan@nssc.ac.cn)
National Space Science Center
Yawar Hussain
University of Liège
Le Cao
Guiyang University
Dandan Cheng
China Research Institute of Radio Wave Propagation

Research Article

Keywords: Ground penetrating radar (GPR), karst catchment, subcutaneous structure, application potential evaluation

Posted Date: October 26th, 2022

DOI: https://doi.org/10.21203/rs.3.rs-2184895/v1

Version of Record: A version of this preprint was published at Environmental Earth Sciences on October 5th, 2023. See the published version at https://doi.org/10.1007/s12665-023-11200-x.

Abstract

The epikarst together with its soil stocks (subcutaneous structure), resulted from the dissolution and weathering of soft rocks, are crucial to the fact that they may contribute to the canopy growth and can significantly influence the ecological restoration and organic carbon sequestration. For the delineation of these ecological significant karst features, ground penetrating radar (GPR) seemed to be a promising technique because of its noninvasive, cost-prohibited and lesser labor-intensive operations. However, the landscape heterogeneity, connection between surface morphology and underground environments and high vegetative endemism making karst as a complicated environment for any geophysical application. Same is the case with the GPR applicability in SW Chinese catchment as it is affected by numerous features such as epikarst slope, peak-cluster depression, tree trunks and roots, precipitation and moisture contents as well as proximity to high voltage power lines. Considering these factors, the present study analyzes the GPR data acquired at the sites representing each of these aforementioned features. The analysis includes calculation of GPR attributes as average energy, coherence and total energy together with the forward calculations wherever required. Tilt signals from surrounding hills mix with the tilt signals from subsurface inclined interfaces in a GPR image. The information of soil-rock distribution above epikarst in the slope is difficult to obtain completely for GPR. The interpretation of epikarst bottom boundary faces two possibilities considering the affects of moisture. The affects of tree trunks and roots and strong electromagnetic fields of high voltages lines make the GPR data interpretation about subsurface soil-rock structure high difficult. The soil moisture greater than ~ 30% makes GPR inapplicability. These site-specific findings are used for the generalized GPR application potential zonation in the typical SW Chinese catchment (the central Guizhou plateau). The findings of the present study may prove as a reconnaissance and an application paradigm for the future GPR utilities in complex karst characterization especially, in SW China as well as the areas having similar karstic conditions.

1. Introduction

The epikarst resulted from the dissolution of carbonate rock, is distributed at the intersections of the Earth's lithosphere, hydrosphere, biosphere and atmosphere, which plays a vital role in regulating the natural habitat, supporting the economy and providing ecological services (Yang and Zhang, 2014). The soil stock of epikarst, as a source of vegetation growth, are key to evaluate ecosystem restoration through organic carbon sequestration at local scale. Hence, the epikarst surveying can significantly influence the research on global carbon, water and calcium cycles.

Nowadays, the karst areas of China have become one of the regions in the world where vegetation coverage and biomass have increased significantly (Brandt et al. 2018; Tong at al. 2018). The karst area of southwest (SW) China is one of the largest karst concentrated areas in the world, and is special for its high landscape heterogeneity, connection between surface morphology and underground environments (fauna and speleothems) through dualistic hydrological system, and high vegetative endemism (Zhang et al. 2017). The soil tocks have been depleted in comparison with the ancient times however, rate of soil weathering is much slower than those of other areas (Zhang et al. 2009). The soil in the epikarst has high

degree of heterogeneity and indented soil-rock interface making it a complicated environment especially, for geophysical applications.

The noninvasive, cost prohibited and less intensive labor characterization of subcutaneous structure that may constitute of the soil stock and the epikarst itself, is one of the significant research aspects of karst studies. In this regard, GPR has the advantage to be used as an effective geophysical technique for the subcutaneous stracture investigations, depth of epikarst and geometry of soil stocks (Gizzi and Leucci 2018, Zhang et al. 2011; Cheng et al. 2019). The average depth associated with these features is shallow and thus lies in the detection range of GPR making it a practical technique to be used in karst explorations as recommend in literature (ref?). The studies of GPR application included the signal responses and interpretation of epikarst and surface soil in some typical transections and sites (Zhang et al. 2011; Li et al. 2015; Han et al. 2016; Gao et al. 2020). Previous studies mainly focus on the interpretation of the subsurface targets and the effects of karst features on GPR exploration have not been discussed or evaluated at a catchment scale.

In terms of the macroscopic or catchment scale study, the use of GPR for soil surveys was successfully demonstrated (Johnson et al. 1979) and for updating soil surveys in Florida (Schellentrager et al. 1988). Doolittle et al (2003, 2007, 2010) developed and later revised GPR soil suitability map based on the field observations made throughout the USA, the national soil attribute data, and the observed responses from the antennas with center frequencies between 100 MHz and 200 MHz. This GPR soil suitability map highlights the expected penetrating depth of different areas of USA by six levels from high to low. The map just focused on the influence of soil properties to GPR signal propagation, not considering the influencing factors generated by the topography and vegetation.

The karst areas of SW China present unique features and topography making the karst catchment complicated and a challenging environment for GPR applications due to the multiplicity of influencing factors. Any successful GPR application to karst landform is therefore a function of several geomorphologcial, geological, climatological and anthropogenic factors. Hence, the present study was carried out to delineate the effects of these features on GPR results. In the first stage, using results from the five experiment sites in the Houzhai catchments of Guizhou, China, the effects are studied. In the next stage, the present study proposes a ranking criterion based on field observations, DEM, and vegetation map for evaluation of GPR application potential in the subcutaneous structure analysis. Additionally, the GPR application paradigm for complicated karst catchment has also been recommended for any future geophysical applications.

2. Study Area

The Houzhai catchment is located in south of Puding county, and belong to heartland of karst area of SW China. This area has western ocean pacific subtropical monsoon humid climate, May to October is classified as the rainy season, accounting for 83–88% of the total annual precipitation (Cheng et al. 2019). The red clay (terra rossa) is the main soil type found in the area which is formed as a result of

carbonate dissolution under local climatic conditions (Zhou et al. 2012). The karst landforms are well developed leading to the formation of typical karst surface and subsurface hydrogeological structure in the catchment.

The Houzhai catchment is located in the watersheds of the Pearl River and Yangtze River systems. The catchment terrain presents a southeast-northwest elevation gradient. Both surface and subsurface rivers originate in the east of the catchment, flow to the northwest, and eventually merge into the Sancha River in north of Puding country, eventually flowing into the Yangtze River. From the upstream to the downstream, a change in geomorphic features occur as peak cluster depression, peak cluster valley, peak forest basin and peak forest plain (Fig. 1). Most slope area of the peaks and hills are grown with forest, shrub or grass. Most flat area of the depressions, valleys and basins are farmland.

In the initial stage, a detailed investigation using the literature and Google imagery has been carried to identification the potential study sites where GPR influencing indicators are well exposed and are easily reachable. Based on these reconnaissances, the GPR experiments have been executed. Additionally, the GPR forward calculation have also been excused where required. Numerous different sites in the catchment were chosen for the field observations. Through compare, the results of five sites can reflect general GPR features under different influencing factors. The positions of five sites are in the DEM (Fig. 1) and the corresponding analysis are discussed in the following.

3. Methods

3.1 Forward modeling

The GPR forward modeling method discussed in this paper is the finite difference time domain (FDTD) technique. The details of GPR FDTD source codes used were provided by Irving and Knight (2006). The GPR forward was applied to demonstrate the sources of tilt signals in GPR data acquired from the peak cluster depression.

3.2 GPR attributes

The conventional processes of raw GPR data must be done before extracting GPR attributes data. The ReflexW software was used for these processing steps as direct wave removal, zero drift elimination, amplitude gain, horizontal signal interference removal, bandpass filtering, data smoothing. F-K filtering method is to transform the GPR data to the frequency wave-number domain for suppressing or eliminating the interference signal which is not easy to process in the time space domain (Jol, 2009). The F-K filtering can be done by the ReflexW software but not necessary for the GPR data without coherent signal interference. The details can be found elsewhere (Gao et al. Under review)

GPR attribute analysis can be seen as the last data processing step prior to the interpretation. The average energy and coherence attributes are extracted to aid in interpretation of the soil-rock interface through the analysis of important features in the signals.

The average energy attribute is defined as the average value of the sum of the squared amplitude value within a fixed time window in a single trace (Gao et al. 2020). All energy values are positive and can magnify the contrast of strong and weak amplitude areas in GPR image. Thus, this attribute can be applied to reflect the position of soil and rock by showing energy contrast of signals.

The coherence attribute quantitatively describes the waveform similarity of adjacent traces (Bahorich and Farmer 1995). This attribute highlights the waveform information by removing the energy feature of signals and its value lies in the range of 0 to 1. High value indicates strong similarity between traces, and vice versa. This attribute can be also applied to reflect the position of discontinuities, such as cracks, faults, etc.

4. Results And Discussions

4.1 Karst slope

The primary structural feature of the karst slope is that epikarst has many fissures filled with soil but the lower bedrock is complete with little fissures (Al-fares et al. 2002). Gao et al. (2020) provided additional evidences of the primary features by applying GPR attributes in analyzing two typical epikarst transects, the rock and soil media of the karst slope are generally exposed to the surface. The interface of soil and rock is indented in the epikarst (Fig. 2). The GPR equipment with 500 MHz shielded antenna was used to detect this slope transect.

Compared to the soil medium, the energy attenuation of electromagnetic signal propagating in the rock medium is slower. Thus, the amplitude energy of signals reflected from rock is stronger for the same depth in soil. The energy attribute can be applied to interpret the soil and rock distribution of epikarst in the valid signal region (Gao et al. 2020). Different from previous interpreting perspective of the slope, the present study utilizes the energy attribute to interpret the lateral and vertical extents of the fissure soil in the epikarst. It can be seen in Fig. 3 that the lateral position of soil exposed to surface is generally corresponding to low energy value and rock to high energy value. But from the vertical perspective, the confirmation of soil depth and indented soil-rock interface delineation is challenging and depending on the energy contrast of GPR data (Fig. 3a).

Additionally, the bottom boundary of epikarst can be interpreted well by the general interface of valid and invalid signals reflected by the coherence attribute. The reflection signals of the layer C under the epikarst exclude the possibility of GPR pulse signal attenuating to zero when propagating to the epikarst bottom boundary (Fig. 3). What if the reflection signal of layer C can’t be seen due to high water content of subsurface media? It would become difficulty to interpret the epikarst lower boundary. Two possible situations can be plausible. One situation is the pulse signal energy attenuates to zero or the lever of random noise before transmitting to the epikarst bottom, thus the interface of valid and invalid signal regions just reflects the maximum penetrating depth. Another situation is the triggered signal attenuates to zero or the lever of random noise between epikarst bottom and the lower layer C. The boundary of valid

and invalid signal regions reflects actually the epikarst lower boundary, but lacking key evidence to prove it. Therefore, it can be concluded that incomplete subsurface information about karst slope can be acquired or interpreted by GPR.

4.2 Peak cluster depression

As one common geomorphic unit in karst area, peak cluster depression consists of the peak cluster hills with steep slope and uneven relative heights and the depression with different sizes and different shapes (Gao et al. under review). The soil-rock interface under the depression can't be completely vertical or horizontal because of the great topography variations in karst area as concluded from numerous previous field observations. The inclined interface under depression should be common. On the other hand, Chen et al (2006) found that the depression soil moisture content changed greatly in the depth range of 0 ~ 30 cm at one peak-cluster depression in Guangxi karst area. The conductivity increases with the increase of soil moisture content (Campbell, 1990). To study the GPR application effect in peak-cluster depression, Gao et al. (under review) carried out this work by forward modelling and actual data analyze in detail.

The GPR forward research about the depression exploration highlighted the factors of surrounding hills, inclined soil-rock interface and soil conductivity (Fig. 4). Through several times of numerical modelling with different conductivity parameters setup, the forward result demonstrates that the tilt signals in GPR image contain the reflection waves both from the hills and the underground inclined interface as long as the soil conductivity is appropriate (Gao et al under review).

The field observations of GPR data were acquired from the Zhongba depression in Houzhai catchment by unshielded 50 MHz RTA (Fig. 5). Several tilt signals are obvious in the radar image (Fig. 6). The real situation of the peak-cluster depression is much more complicated than that of the forward model. The F-K filtering method was applied to eliminate the tilt signals. Further analysis of the measured data can be seen in the study work of Gao et al (2020) and Gao et al. (under review). The auger verification demonstrated that the retained horizontal signals can provide information of the internal soil layers in depression while information about the inclined interface information is lost (Gao et al 2020; Gao et al. under review). Therefore, partial information about depression soil can be acquired using low frequency antenna because of the interference from the surrounding hills.

Contrasted with the previous studies, we did more GPR work in the depression with the 500 MHz shielded antenna at the same detection line and the result is shown as Fig. 7. Though the measured data is not affected by the reflection from hills, the radar wave of high frequency can't penetrate to the bottom of depression soil. The valid signals just occupy the previous 20 ns, less than 1 meter of soil depth. High frequency antenna is not suitable for interpreting depression soil depth.

4.3 Tree trunks and roots

Many regions of the Houzhai catchment are covered by forest trees which may reflect the presence of large soil stocks in the karst. Two such forest sites (site-1 and site-2) were chosen, site-2 lies next to the largest water reservoir in the catchment (Fig. 8) for GPR survey using the 50 MHz RTA.

Contrasting to the GPR images of these two sites (Fig. 9), the valid signals of the site 1 can last more than 300 ns, while that of the site 2 last less than 200 ns. This phenomenon indicates that the site 2 has higher soil conductivity than the site 1. On the other hand, lots of tilt signals can be seen in the images. Most of the tree trunk diameter is more than 10 cm which reaches the resolution of low frequency antenna. According to the analogy derivation of the forward study result of the peak-cluster depression, we speculate that the tilt signals include the waves reflected by the tree trunks or the subsurface inclined interface. Additionally, many experts study tree roots architecture by GPR signal response (Zajícová and Chuman 2019). The GPR data should contain the waves reflected by tree roots. The complicated tree roots system makes the interpretation of tree land soil structure and epikarst depth more difficult. Therefore, we deem that the accurate information of soil distribution in karst forest land is high difficulty to obtain by GPR due to the mix of tree trunks and roots reflection signals. The epikarst survey over the woodland soil layer is challenged by the presence of more prominent influencing factors as deeper soil with high moisture contents.

The high frequency antenna is more convenient to detect the roots system (Alani and Lantini 2020). Though the reflection signals of the trunks have been shielded, the complicated roots system still makes the soil and epikarst interpretation difficult from the data acquired using 500 MHz antenna.

4.4 Rainfall and soil moisture

To make sure the detection effect of the maximum soil water content, one paddy land near the catchment was chosen (Fig. 10). We made the GPR survey with 50 MHz RTA few days after the rice harvest completion. The rice field water had just seeped into the ground, which increase the soil moisture content along the depth. The surface soil moisture content is more than 30% measured by instrument.

Analyzing the measured GPR data and its coherence attribute (Fig. 11), we found the majority of signals have weak amplitude and low similarity, which fit the features of random noise interference (Jol 2009). This suggests that radar waves almost cannot penetrate soil layer with more than 30% moisture content.

4.5 High voltage power lines

Three high voltage power lines pass through the Houzhai catchment in our field observations. High voltage transmission lines generate strong electromagnetic fields around the lines. Cheng et al (2010) have shown that low frequency GPR is affected by high voltage lines within the 100 meters range. In order to understand the impact of strong electric field on GPR data acquired by unshielded antenna, one grass land under high voltage power lines was chosen for the test (Fig. 12). After the conventional process, the data was found affected by strong signal interference which has high similarity (Fig. 13). After the F-K filtering, although the interference signal with strong amplitude is suppressed, the coherence

attribute image shows that the interference signal with high similarity still exists (Fig. 14). Therefore, while evaluating the potential of GPR survey one cannot ignore the influence of the high voltage lines.

5. Application Potential Evaluation

The catchment scale application potential evaluation of GPR acquired using 50 MHz RTA and 500 MHz shielded antenna in detecting karst surface structure in the Houzhai catchment is carried out. The catchment is initially divided into three regions as low, moderate and high potential, based on field observations, the topography (Fig. 1) and vegetation cover data (see Appendix). Different potential degrees reflect the reliability of GPR data interpretation for soil distribution and epikarst depth by considering surface and subsurface influencing factors. Table 1 summarizes the findings of the present study as well as inferred from literature review.

Table 1
the potential degree evaluation of GPR applied to the Houzhai catchment

Potential degree	Corresponding geomorphic region and land use	Influencing factors	Effect of interpreting soil distribution for 50 MHz RTA and 500 MHz shielded antenna	Effect of interpreting epikarst depth for 50 MHz RTA and 500 MHz shielded antenna
low	Forest land, High voltage line within 100 meters range	Tree trunk, tree root, high-voltage lines, moisture content, soil thickness	Bad effect for two kinds antennas, Great multiple solutions, High difficulty to interpret due to signals overlap of trunk, root and inclined interface reflection Poor methods to filter interference	Bad effect for two kinds antennas, Great multiple solutions, High difficulty to interpret with further considering the soil thickness and moisture content, High difficulty to confirm the epikarst depth,
Moderate	karst slope, bottom of peak cluster depression, bottom of peak cluster valley	Moisture content, Soil layer thickness, Hills reflection	Interpret the soil structure in karst slope is moderate difficulty for 500 MHz but high difficulty for 50 MHz Moderate difficulty in the depression and valley for 50 MHz RTA due to the tilt signals overlap, 500 MHz antenna is not suitable in the depression and valley due to the soil thickness and moisture content	Shallow karst cave or pipelines under karst slope can be possibly detected by 50 MHz, more difficulty for 500 MHz; Interpretation difficulty of epikarst depth increases from top to foot of karst slope for both antennas; Reflection signals of epikarst inclined interface under valley and depression can overlap with the hill reflection signals for 50 MHz if soil layer is not too sick.
high	Basin, plain, agricultural land use	Soil layer thickness, Moisture content	Soil layer depth and soil-rock interface can be quantitatively interpreted for 50 MHz RTA. The accuracy can be verified by auger. High difficulty for 500 MHz to penetrate soil bottom	High difficulty to interpret epikarst under the soil layer for two kinds antennas; Epikarst information may not be acquired when soil thickness is close to 4 meters for 50 MHz RTA, shallower for 500 MHz

Low potential degree regions (e.g., forest lands and high voltage lines) are the areas where GPR data show multi-source interference as compared to signals of interests leading to difficulties in interpreting the soil and epikarst. Most of the forest lands are mainly distributed in the peak-cluster depression and peak-cluster valley of the catchment while some of forests are also grown at the flat sites. The

influencing factors include tree trunks, roots system, high voltage lines, soil layer depth and moisture content. The diameter of tree trunk is usually more than 10 cm, reaching the resolution of the 50MHz and 500 MHz antennas. The effects of tree roots on GPR results as reflection of radar waves, have been documented in literature (e.g., Tardío et al. 2016; Alani and Lantini 2020). The reflection from trunks and roots are mixed with those from subsurface media, making the GPR results obscure and separation of real sources of either horizontal or tilt signals is difficult. Tall and dense growing trees imply a large amount of soil with a relatively large thickness. Whether radar wave can penetrate the maximum depth of soil or not has great uncertainty, especially for high frequency antenna. The electromagnetic field generated by the high voltage lines gives the GPR data great interference which is difficult to eliminate.

Moderate potential degree regions are the areas where partial information of the target is acquired while rest is lost because of the overlaping or attenuation of signals. The peak-cluster depression bottom, the bottom of peak-cluster valley and slope without forests can be classified into this catagory. The influencing factors include reflections from hills, soil thickness and moisture content.

In the first stage, the effects of karst slope on GPR results vary with the frequency antennas used as well as soil distribution on the slope. The general feature of karst slope is, the soil distribution becomes deeper and heterogeneous from upslope to downslope. The epikarst depth also increases gradually in downslope direction. The shallow and discontinuous surface soil is available for low frequency antenna to detect caves (Čeru et al. 2018; Hussain et al. 2020). Generally, shallow caves or pipelines are deeper than epikarst lower boundary and could be detected in favorable conditions as thinner and dry soil. The reflection from caves or pipelines can also account for GPR signals penetration till epikast bottom. But it is difficulty for 50 MHz data to interpret the upslope fissure soil distribution due to low resolution and little soil distribution. As for the 500 MHz (high frequency) antenna, the achievement of the interpretation of slope epikarst bottom requests lower moisture theoretically. The GPR coherence attribute is beneficial in interpreting the valid and invalid signals interface, which may correspond to the epikarst bottom (Gao et al. 2020). However, the level of difficulty in interpreting epikarst bottom depth increases from upslope to downslope due to the increase of soil thickness and moisture content.

Secondly, the use of low frequency antenna is recommended for the exploration of soil layer bottoms in peak-cluster depression and valley. In terms of unshielded 50 MHz RTA, the signals reflected by hills overlap with the signals reflected from the subsurface inclined interface due to the depression and valley close to hills, making difficult to accurately confirm the exact source of tilt signals. The tilt signals can be eliminated by F-K filtering, and the retained signals can reflect the depth of soil lateral layers and soil-rock interface in the depression and valley through extracting the average amplitude attribute and coherence attribute (Gao et al. under review). Unfortunately, the information of the inclined interface has been lost. The surface of depression and valley is usually entirely covered with the soil layer which is deeper than that of soil found on slope. Additionally, the bottom of karst peak-cluster depression and valley is a sink for the rainfall and runoff from the adjoining areas. Therefore, the these are the region of high soil moisture contents than that of slope soil. It is challenging to detect the epikarst depth under the depression and valley using low frequency antenna.

Summarizing the above GPR interpreting effects of high and moderate regions with high and low center frequency antennas, we sum up above results and draw the key information into one simple sketch as shown in Fig. 15.

High application potential is the region where GPR information is solely obtained from the subsurface structures without having any influence from the external factors as explained above. This region corresponds to the basin and plain of the catchment, excluding the sites covered by forest. Results of GPR data acquired from this region have high reliability in the soil and epikarst delineation. The soil distribution can be interpreted by analyzing the average amplitude attribute and coherence attribute and result accuracy can be verified by drilling. However, GPR acquiring the depth information of epikarst under relatively thick soil layer is most difficult. The limited thickness of soil layer can be referred to the example of the Zhongba depression. The thickness and water content of soil layer are usually higher than those of slope. The thickness of soil layer in the Zhongba depression is ~ 4 meters (Gao et al. 2020). The measured data was acquired in the premise of no rainfall event and hot weather lasting more than a week. The 50 MHz antenna just detected the maximum depth of the soil layer and did not receive the echo signals of the deeper epikarst. Thus, we simply consider the soil thickness close to 4 meters is not conducive for low frequency antenna to obtain the structure information of epikarst. As for the 500 MHz antenna with high resolution, its requirement for the soil thickness is much shallower.

The above information is summarized in one rough map about the application potential evaluation of GPR application in the Houzhai catchment based on the DEM, the vegetation data and locations of high voltage lines (Fig. 16).

Considering the seasonal variability of climatic conditions in the Houzhai catchment, the soil moisture content changes from low to high with dry to rainy seasons, receptively. The rainy period is not a good time for GPR survey because of high soil conductivity. We recommended the months of October and November as the best time for GPR acquisition in the catchment. On the one hand, this period is at the end of the rainy season and the soil in dry season has relatively low moisture content and conductivity (Yang et al. 2019). On the other hand, the majority place of the low uncertainty region is the farmland. October and November are the period between the summer crop being harvested and the winter crop not fully planted. It is also a good period to from the view of not destroying crops.

6. Gpr Application Paradigms

The potential evaluation results show that GPR technology is beneficial to the detection of partial subsurface structures in the karst catchment. On the basis of summarizing the exploration effects from the macroscopic view, we further propose an application paradigm diagram of GPR methods to karst catchment. The paradigm provides one pattern of GPR applied to karst area and help investigators considering the order of the influencing factors. Before putting out the paradigm, we summarize some relevant experiences of other scholars in electrical methods and seismic exploration.

Other geophysical methods, such as EM induction, ERT and seismic exploration, are also applied in karst area. GPR, electromagnetic (EM) induction and electrical resistivity tomography (ERT) all realize the detection purpose based on the electrical difference of subsurface media. The integrated use of EM induction and GPR can increase the confidence of interpreters in the interpretive results about karst structures (Doolittle and Collins 1998). ERT can give the characterization of soil-rock interface and sinkhole from another perspective comparing with GPR (Carbonel et al. 2014). ERT can delineate the general soil-rick interface of the thick bedded limestone and dolostone environments, but can't delineate the interface when the laminar bedded limestone has great moisture retention (Cheng et al 2019). The high moisture content of the medium greatly reduces the accuracy of electrical methods.

Seismic exploration utilizes the elasticity and density difference of subsurface media to identify the underground structure by triggering seismic waves, which consist of P-wave, S-wave and so on. According to the study results of Carcione et al (2003) and Ding et al (2014), the velocity of P-wave decreases with increasing soil water saturation and the attenuation of P-wave is larger in dry soils than in wet soils. Seismic exploration methods are more suitable for the high moisture content conditions. To overcome the limitations of electrical and electromagnetic techniques, seismic methods have been successfully applied to monitoring the subsurface water levels depth (Desper et al 2015; Pasquet et al 2016). Because of the different soil moisture content, ERT has higher accuracy detecting soil depth at upslope and seismic method has higher accuracy at downslope (Coulouma et al 2012). The field survey results in Europe karst regions concluded that the combination of seismic methods and electrical methods can be considered as powerful tools for mapping complex karstic environments (Šumanovac and Weisser 2001; Valois et al 2011). Seismic refraction methods can give additional valuable information of deeper targets of more than 100 m, which is very difficult for GPR or ERT. Combining the seismic data and electrical data, Guo et al (2021) analyzed the geological structure, karst cave and fissure karst water in 500 m depth underground in Fuling area, Chongqing Municipality, China. Seismic explorations are less applied than GPR and ERT in the karst area of SW China. We suggest the more application of seismic to the karst catchment can overcome the spatial and time limitations of electromagnetic methods and give more information about deeper targets.

At last, we summarize the previous experiences of geophysical exploration in order to recommend other applicable methods for the case that GPR is not suitable for detection. Figure 17 shows the application paradigm of GPR in karst catchment proposed by this paper. The paradigm aims at the subcutaneous structure, mainly for the surface soil and epikarst. This paradigm provides each step of the GPR field investigation process, which reflects considering the order of various influencing factors in the survey. First, the detection point or line should be designed 100 meters away from the high voltage line. Secondly, weather should be considered during detection. If there is rainfall and the water content of the medium exceeds 30%, GPR is not suitable at this time, and seismic exploration is recommended. In case of no rainfall, the vegetation factors we should consider whether the survey sites are covered by forests. If covered by forest, it is very difficult for GPR to carry out exploration. For areas not covered by forest, we need to further consider the factors of geomorphic units. Three geomorphic units are mainly considered: slope, the bottom of peak-cluster depression or valley, plain and basin or other flat areas with little surface

undulations. The different geomorphic units need to be analyzed from different angles. Slope land is divided into upslope and downslope, further. The upslope is suitable for detection, while the downslope is more difficult for GPR and we can combine with seismic technology. The detection of depression or valley must take mountain reflection interference into account. The flat areas are suitable for GPR detection. Three ways can be used to verify the accuracy of interpretation of measured GPR data: drilling, sections survey, and comprehensive evaluation by comparing with electrical methods and seismic explorations.

7. Summary

In view of the lack of macro evaluation of GPR applied to karst catchment, this paper summarized the detection effects of GPR field observations at different sites in the Houzhai river catchment, a typical catchment in karst area of SW China. Additionally, we combined with geomorphology, vegetation, moisture content, high voltage lines and other influencing factors, and evaluated the application potential faced by GPR in detecting surface soil and epikarst from the catchment scale. The application potential degree evaluation answers the reliability of GPR data interpretation results acquired in different regions of karst catchment. What's significant, we developed initially the corresponding potential degree map of the Houzhai catchment. Additionally, we proposed one application paradigm of GPR methods in karst areas. We've come up with one significant conclusion: the potential degree of GPR applied in the Houzhai catchment can be roughly divided into three different regions: high, moderate and low. The corresponding potential map is expected to help investigators who are unfamiliar with GPR or the karst environment to have a macroscopic perspective.

This study is just initial and some complicated factors are ignored. Future relative study should consider more contents such as applying more different frequency antennas, more detailed geomorphological division, more field observations and forward works.

Every method has its advantages and drawbacks. Wet soil is conducive to the propagation of seismic waves, not conducive to that of electromagnetic waves, while dry soil is just the opposite. In terms of the karst catchment survey, the combination of seismic and electromagnetic methods can overcome the shortcomings of each other and expand the application range. The potential and difficulty of seismic methods and other geophysical methods applied comprehensively in karst catchment scale is worthy of investing more research, which can provide macroscopic technical support for the subsequent research about the soil stocks, epikarst depth, caves, subsurface pipelines and so on.

Declarations

Conflict of interest

The authors declare no conflicts of interest.

References

1. Alani AM, Lantini L (2020) Recent Advances in Tree Root Mapping and Assessment Using Non-destructive Testing Methods: A Focus on Ground Penetrating Radar. Surveys in Geophysics 41:605–646. Doi: 10.1007/s10712-019-09548-6
2. Al-fares W, Bakalowicz M, Guérin R, Dukhan M (2002) Analysis of the karst aquifer structure of the Lamalou area (Hérault, France) with ground penetrating radar. J Appl Geophys 51:97–106. https://doi.org/10.1016/S0926-9851(02)00215-X
3. Bahorich M, Farmer S (1995) 3-D seismic discontinuity for faults and stratigraphic features: The coherence cube. The Leading Edge 14:1053–1058. Doi: 10.1190/1.1437077
4. Brandt M, Yue Y, Wigneron JP, et al (2018) Satellite-Observed Major Greening and Biomass Increase in South China Karst During Recent Decade. Earth's Future 6:1017–1028. Doi: 10.1029/2018EF000890
5. Campbell JE (1990) Dielectric Properties and Influence of Conductivity in Soils at One to Fifty Megahertz. Soil Science Society of America Journal 54:332–341. Doi: 10.2136/sssaj1990.03615995005400020006x
6. Carbonel D, Rodríguez V, Gutiérrez F, et al (2014) Evaluation of trenching, ground penetrating radar (GPR) and electrical resistivity tomography (ERT) for sinkhole characterization. Earth Surface Processes and Landforms 39:214–227. Doi: 10.1002/esp.3440
7. Carcione JM, Seriani GS, Gei D (2003) Acoustic and electromagnetic properties of soils saturated with salt water and NAPL. Journal of Applied Geophysics 52:177–191. Doi: 10.1016/S0926-9851(03)00012-0
8. Čeru T, Šegina E, Knez M, et al (2018) Detecting and characterizing unroofed caves by ground penetrating radar. Geomorphology 303:524–539. Doi: 10.1016/j.geomorph.2017.11.004
9. Chen, H., Fu, W., Wang, K., et al., 2006. Dynamic Change of Soil Water in Peak-Cluster Depression Areas of Karst Mountainous Region in Northwest Guangxi. Bulletin of soil and water conservation 20, 136–139. (in Chinese). Doi: 10.13870/j.cnki.stbcxb.2006.04.033
10. Cheng J, Pan D, Li W, et al (2010) Study on the detecting of hazard abandoned workings by ground penetrating radar on srong electromagenetic interference area. Journal of China Coal Society 35(2): 227–231. (in Chinese) DOI: 10.13225/j.cnki.jccs.2010.02.017
11. Cheng Q, Tao M, Chen X, Binley A (2019) Evaluation of electrical resistivity tomography (ERT) for mapping the soil–rock interface in karstic environments. Environmental Earth Sciences 78:1–14. Doi: 10.1007/s12665-019-8440-8
12. Coulouma G, Samyn K, Grandjean G, et al (2012) Combining seismic and electric methods for predicting bedrock depth along a Mediterranean soil toposequence. Geoderma 170:39–47. Doi: 10.1016/j.geoderma.2011.11.015
13. Desper DB, Link CA, Nelson PN (2015) Accurate water-table depth estimation using seismic refraction in areas of rapidly varying subsurface conditions. Near Surface Geophysics 13:455–465. Doi: 10.3997/1873-0604.2015039

14. Ding W, Wu We, Wang C, Wu Z (2014) Propagation characteristics of seismic waves in shallow soil with the unsaturated three-phase poroelastic model. Acta Physica Sinica 63:224301. (in Chinese) Doi: 10.7498/aps.63.224301
15. Doolittle JA, Collins ME (1998) A comparison of EM induction and GPR methods in areas of karst. Geoderma 85:83–102. Doi: 10.1016/S0016-7061(98)00012-3
16. Doolittle JA, Minzenmayer FE, Waltman SW, Benham EC (2003) Ground penetrating radar soil suitability maps. Journal of Environmental and Engineering Geophysics 8:49–56. Doi: 10.4133/JEEG8.2.49
17. Doolittle JA, Minzenmayer FE, Waltman SW, et al (2007) Ground-penetrating radar soil suitability map of the conterminous United States. Geoderma 141:416–421. Doi: 10.1016/j.geoderma.2007.05.015
18. Doolittle J, Dobos R, Peaslee S, et al (2010) Revised Ground-Penetrating Radar Soil Suitability Maps. Journal of Environmental and Engineering Geophysics 15:111–118. Doi: 10.2113/JEEG15.3.111
19. Gao Q, Wang S, Peng T, et al (2020) Evaluating the structure characteristics of epikarst at a typical peak cluster depression in Guizhou plateau area using ground penetrating radar attributes. Geomorphology 364:107015. Doi: 10.1016/j.geomorph.2019.107015
20. Gao Q, Hussain Y, Yang T (under review) A brief analysis of application potential of georadar in karst peak-cluster depression studies. Journal of Applied Geophysics
21. Gizzi FT, Leucci G (2018) Global Research Patterns on Ground Penetrating Radar (GPR). Surveys in Geophysics 39:1039–1068. https://doi.org/10.1007/s10712-018-9475-1
22. Guo S, Zhu J, Wang C, et al (2021) Study on the joint application of electrical and seismic exploration in the investigation of fissure and Karst cave in Fuling area. CT Theory and Applications 30: 49–59. DOI:10.15953/j.1004-4140.2021.30.01.05. (in Chinese).
23. Han X, Liu J, Zhang J, Zhang Z (2016) Identifying soil structure along headwater hillslopes using ground penetrating radar based technique. Journal of Mountain Science 13:405–415. Doi: 10.1007/s11629-014-3279-7
24. Hubbard RK, Asmussen LE, Perkins HF (1990) Use of ground-penetrating radar on upland coastal plain soils. Journal of Soil and Water Conservation, 45: 399–405.
25. Hussain Y, Rogerio U, Welitom B, et al (2020) The Potential Use of Geophysical Methods to Identify Cavities, Sinkholes and Pathways for Water Infiltration. Water 12: 2289. https://doi.org/10.3390/w12082289
26. Irving J, Knight R (2006) Numerical modeling of ground-penetrating radar in 2-D using MATLAB. Computers and Geosciences 32:1247–1258. Doi: 10.1016/j.cageo.2005.11.006
27. Johnson RW, Glaccum R, Wojtasinski R (1979) Application of ground penetrating radar to soil survey. Soil and Crop Science Society of Florida Proceedings 39: 68–72.
28. Jol, H.M., 2009. Ground Penetrating Radar: Theory and Applications. Elsevier Science, Amsterdam.

29. Li L, Xia Y hang, Liu S juan, et al (2015) Modified method for estimating organic carbon density in discontinuous Karst soil using ground-penetrating radar and geostatistics. Journal of Mountain Science 12:1229–1240. Doi: 10.1007/s11629-015-3431-z
30. Pasquet S, Bodet L, Bergamo P, et al (2016) Small-Scale Seismic Monitoring of Varying Water Levels in Granular Media. Vadose Zone Journal 15:1–14. Doi: 10.2136/vzj2015.11.0142
31. Schellentrager GW, Doolittle JA, Calhoun TE, Wettstein CA (1988) Using Ground-Penetrating Radar to Update Soil Survey Information. Soil Science Society of America Journal 52:746–752. Doi: 10.2136/sssaj1988.03615995005200030027x
32. Szuch RP, White JG, Vepraskas MJ, Doolittle JA (2006) Application of ground penetrating radar to aid restoration planning for a drained carolina BAY. Wetlands 26:205–216. Doi: 10.1672/0277-5212(2006)26[205:AOGPRT]2.0.CO;2
33. Šumanovac F, Weisser M (2001) Evaluation of resistivity and seismic methods for hydrogeological mapping in karst terrains. Journal of Applied Geophysics 47:13–28. Doi: 10.1016/S0926-9851(01)00044-1
34. Tardío G, González-Ollauri A, Mickovski SB (2016) A non-invasive preferential root distribution analysis methodology from a slope stability approach. Ecological Engineering 97:46–57. Doi: 10.1016/j.ecoleng.2016.08.005
35. Tong X, Brandt M, Yue Y, et al (2018) Increased vegetation growth and carbon stock in China karst via ecological engineering. Nature Sustainability 1:44–50. Doi: 10.1038/s41893-017-0004-x
36. Valois R, Camerlynck C, Dhemaied A, et al (2011) Assessment of doline geometry using geophysics on the Quercy plateau karst (South France). Earth Surface Processes and Landforms 36:1183–1192. Doi: 10.1002/esp.2144
37. Yang J, Chen H, Nie Y, Wang K (2019) Dynamic variations in profile soil water on karst hillslopes in Southwest China. Catena 172:655–663. Doi: 10.1016/j.catena.2018.09.032
38. Yang J, Zhang C (2014) Earth's critical zone: a holistic frame for geo-environment researches. Hydrgeology & Engineering Geology 41: 98–104, 110. (in Chinese). Doi: 10.16030/j.cnki.issn.1000-3665.2014.03.012
39. Zajícová K, Chuman T (2019) Application of ground penetrating radar methods in soil studies: A review. Geoderma 343:116–129. Doi: 10.1016/j.geoderma.2019.02.024
40. Zhang Z, Chen X, Cheng Q, et al (2011) Hydrogeology of epikarst in karst mountains — A case study of the Chenqi catchment. Earth and Environment 39, 19–25. (in Chinese). Doi:10.14050/j.cnki.1672-9250.2011.01.016
41. Zhang C, Qi X, Wang K, et al (2017) The application of geospatial techniques in monitoring karst vegetation recovery in southwest China: A review. Progress in Physical Geography 41:450–477. Doi: 10.1177/0309133317714246
42. Zhang X, Wang S, Cao J (2009) Mass Balance of Silicate Minerals in Soils and Soil Losses in the Karst Mountainous Regions of Southwest China. 37: 97–102. (in Chinese)

43. Zeng Z, Liu S, et al (2010) Ground penetrating radar principle and application. Publishing House of Electronics Industry, pp54, Beijing. (in Chinese)
44. Zhou J, Tang Y, Yang P, et al (2012) Inference of creep mechanism in underground soil loss of karst conduits I. Conceptual model. Natural Hazards 62:1191–1215. Doi: 10.1007/s11069-012-0143-3

Figures

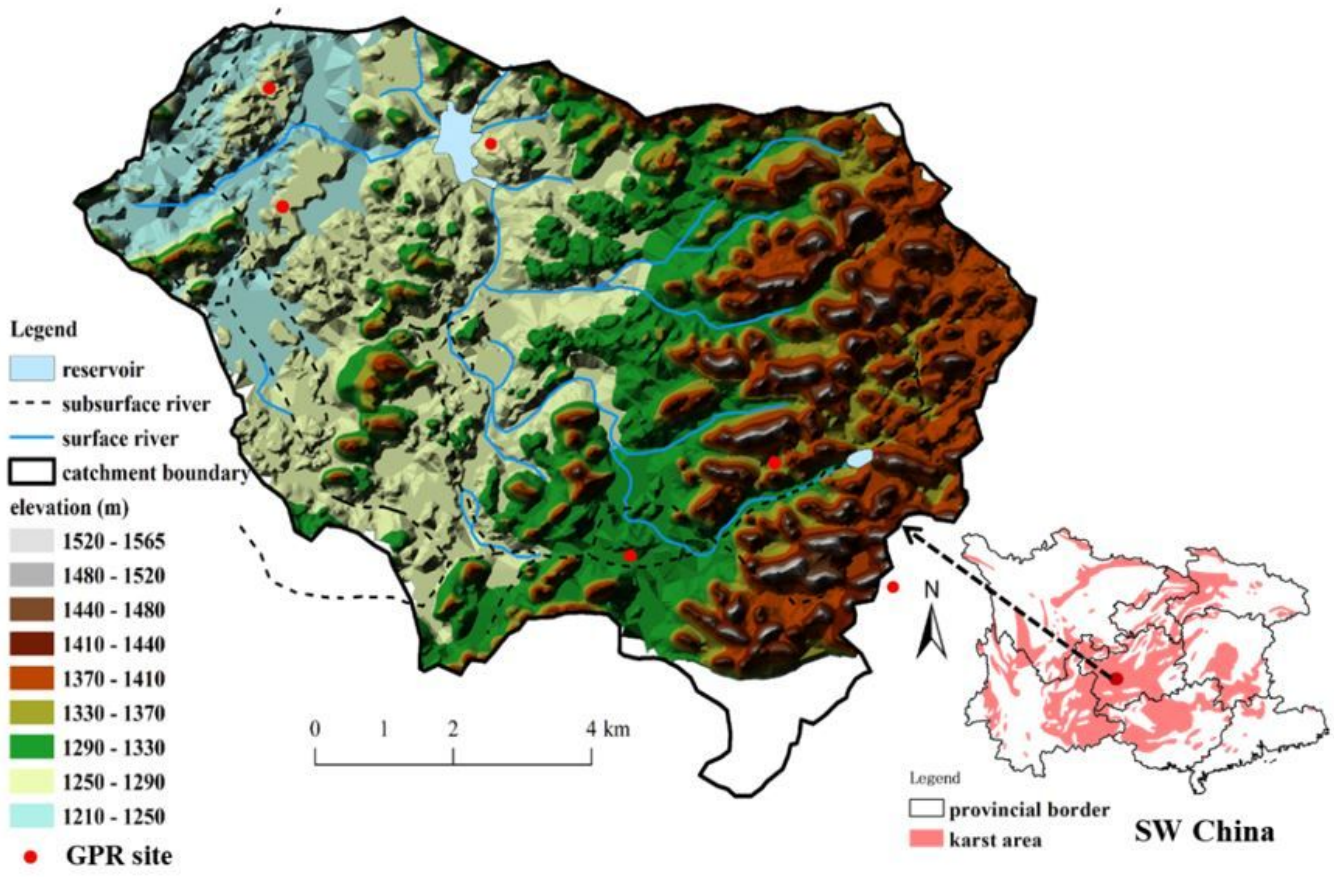

Figure 1

The red dots on the DEM of the Houzhai catchment area marked the GPR acquisition sites along with important hydrological features of interests. The insert shows the SW China map.

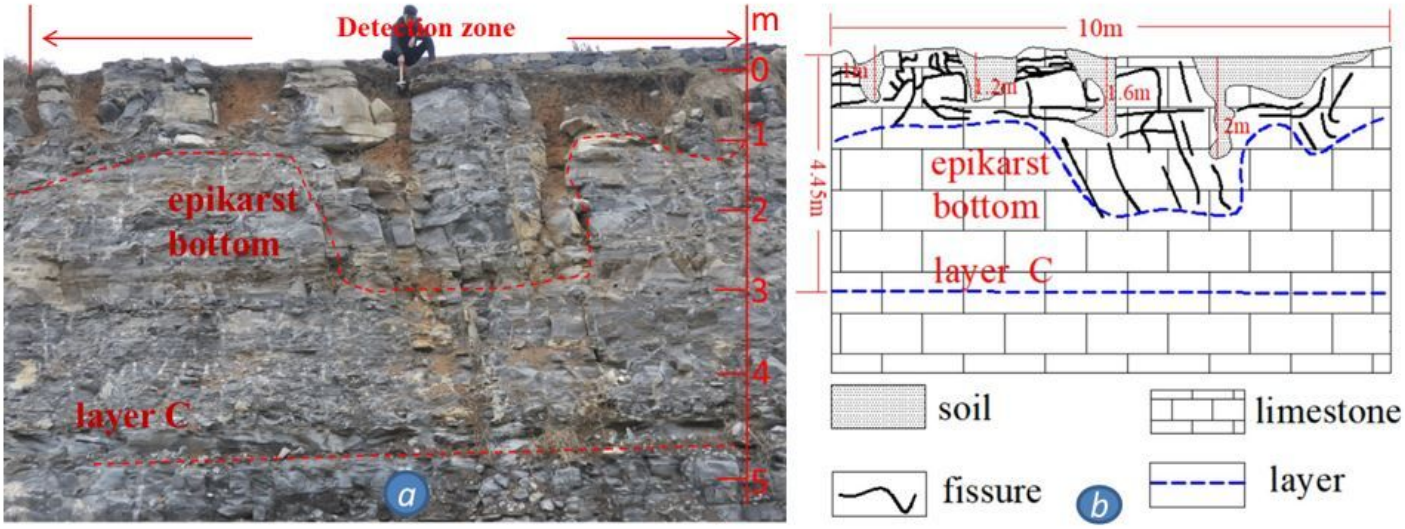

Figure 2

(a) photograph of a typical karst slope. Two red dotted lines are drawn, the upper is lower boundary of epikarst and the lower line is layer C. (b) GPR based driven cross-section showing epikarst indented soil-rock interfaces (revised from Gao et al. 2020).

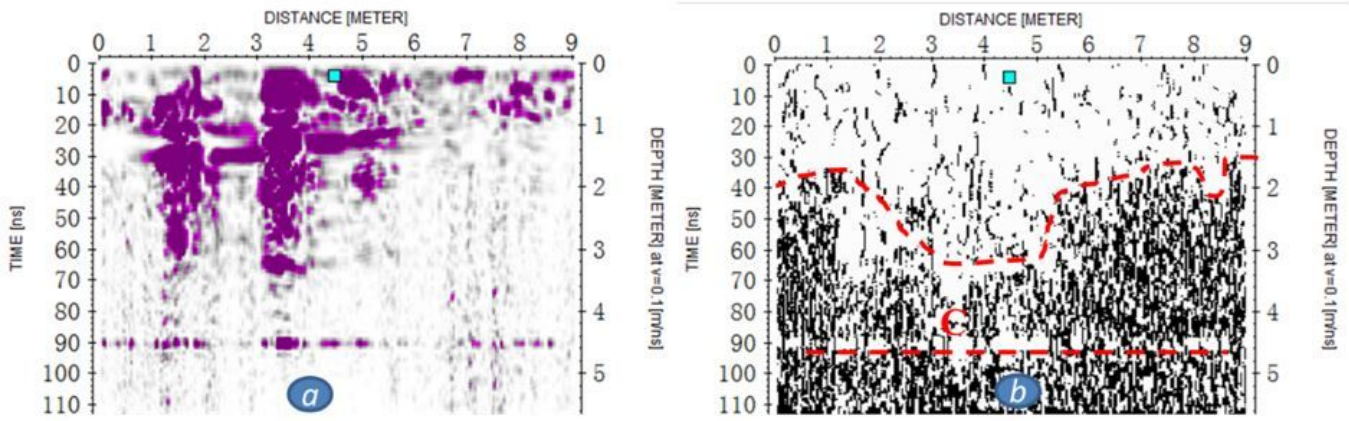

Figure 3

the average energy attribute (a) and coherence attribute (b) acquired on a karst slope adopted after Gao et al. (2020). The bright color of purple is high energy value and dull color of white and grey is low value. The cyan block mark corresponds to position of the hammer in Figure 2a and fissure soil medium. The red dotted line in the right panel draws the epikarst bottom interface interpreted by GPR attribute.

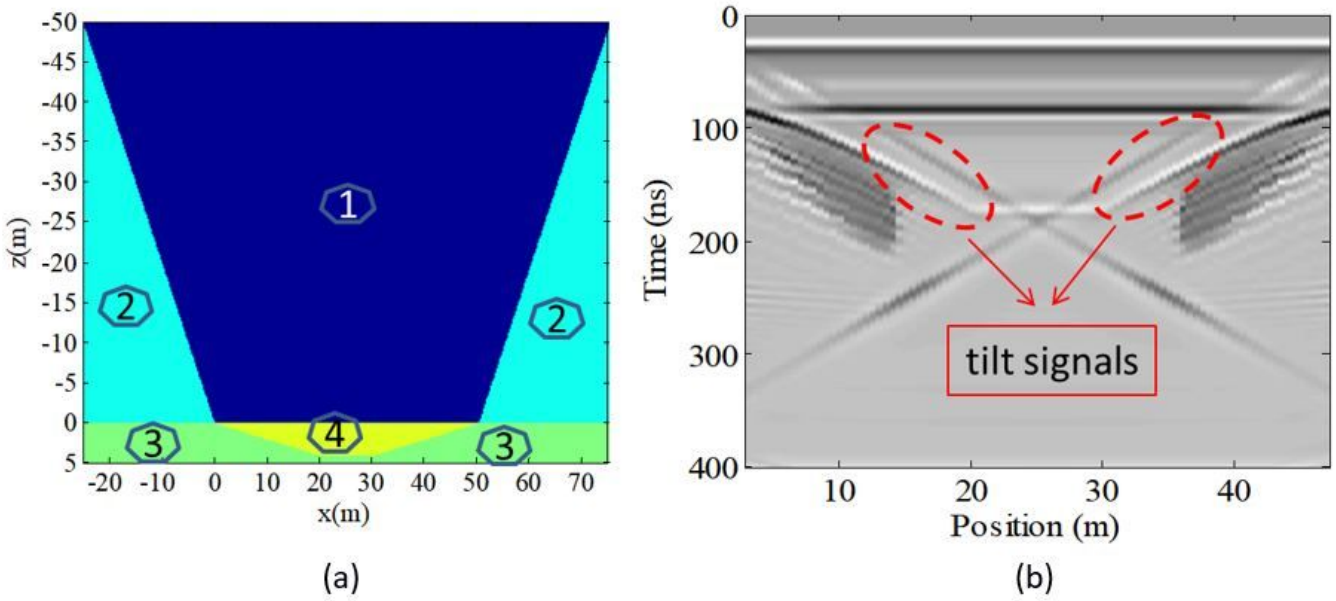

Figure 4

the forward model of peak-cluster depression (a) and its forward result (b) by FDTD. The annotations represent the air, the hill, the bedrock, and the soil of the depression (Adopted from Gao et al. under review).

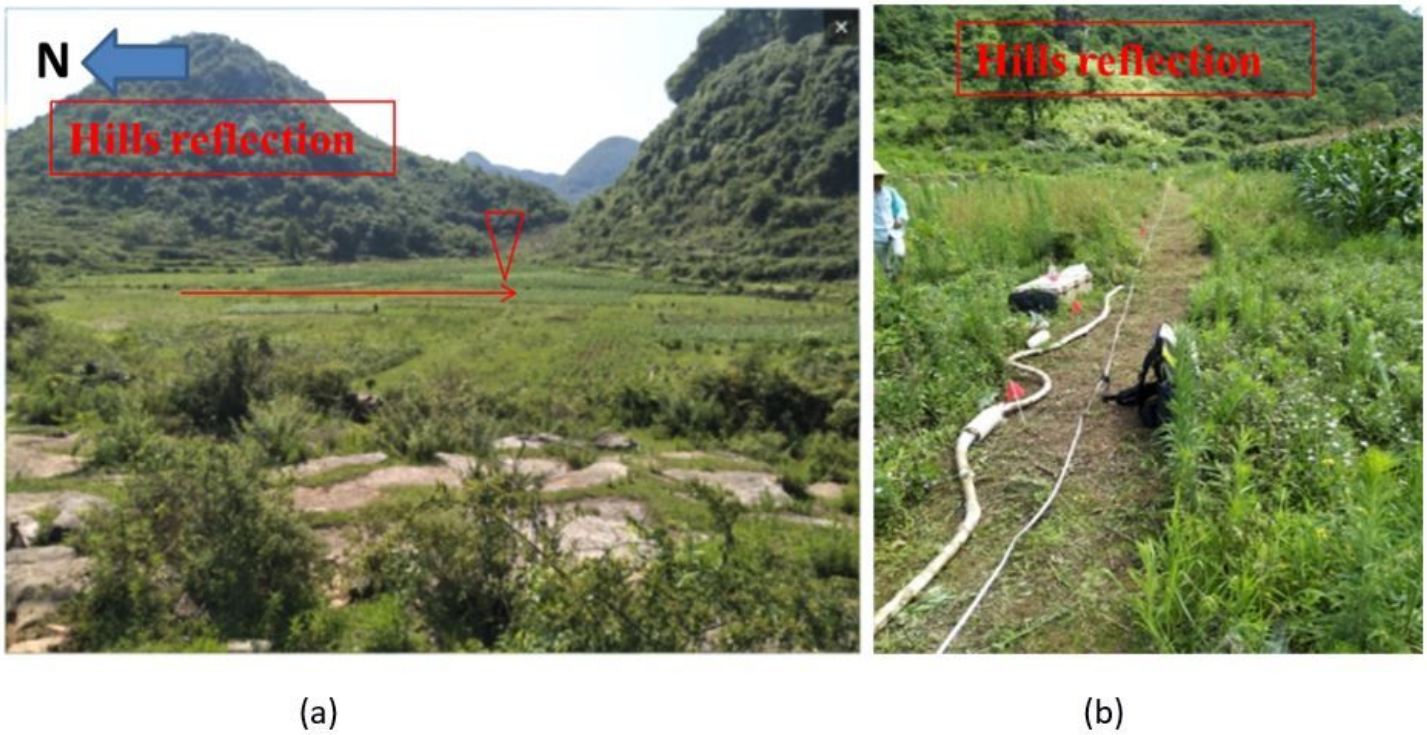

Figure 5

Photosgraphs of (a) Zhongba depression, red arrow marks the GPR survey line and directionand (b) GPR acquisition revised according to Gao et al (2020).

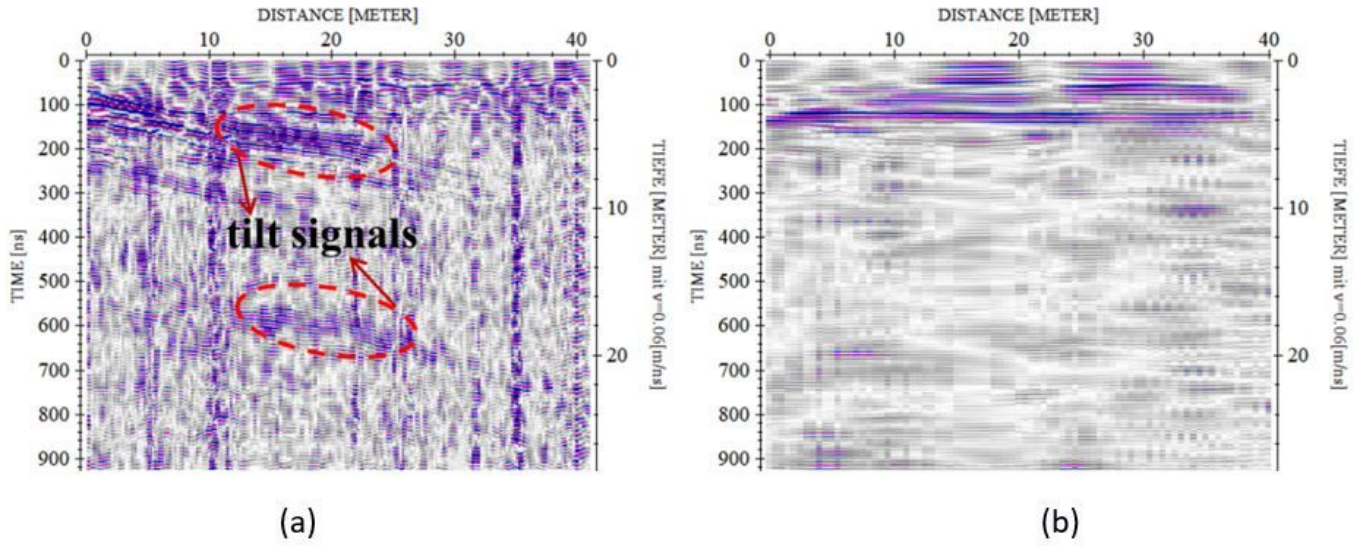

Figure 6

Conventional GPR images of the Zhongba depression (a) and processed applying F-K filtering (b) revised from Gao et al. (under review).

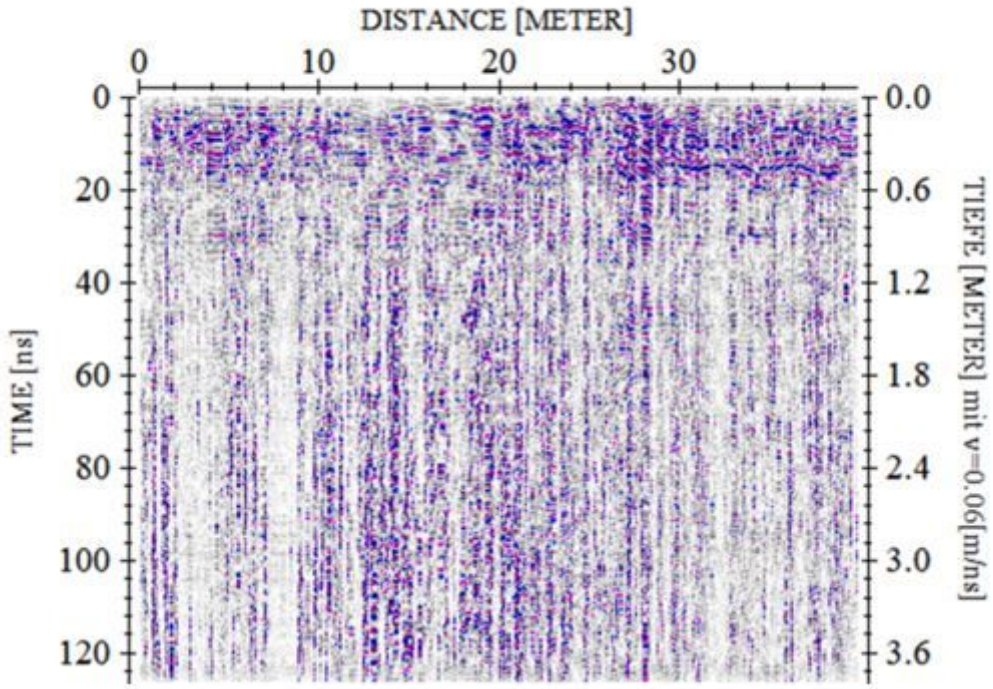

Figure 7

GPR data image acquired by the shielded 500 MHz antenna. The black broken line indicates the soil-rock interface of the depression.

(a) (b)

Figure 8

Site-1 (a) and site-2 (b) of forest land close to a water reservoir

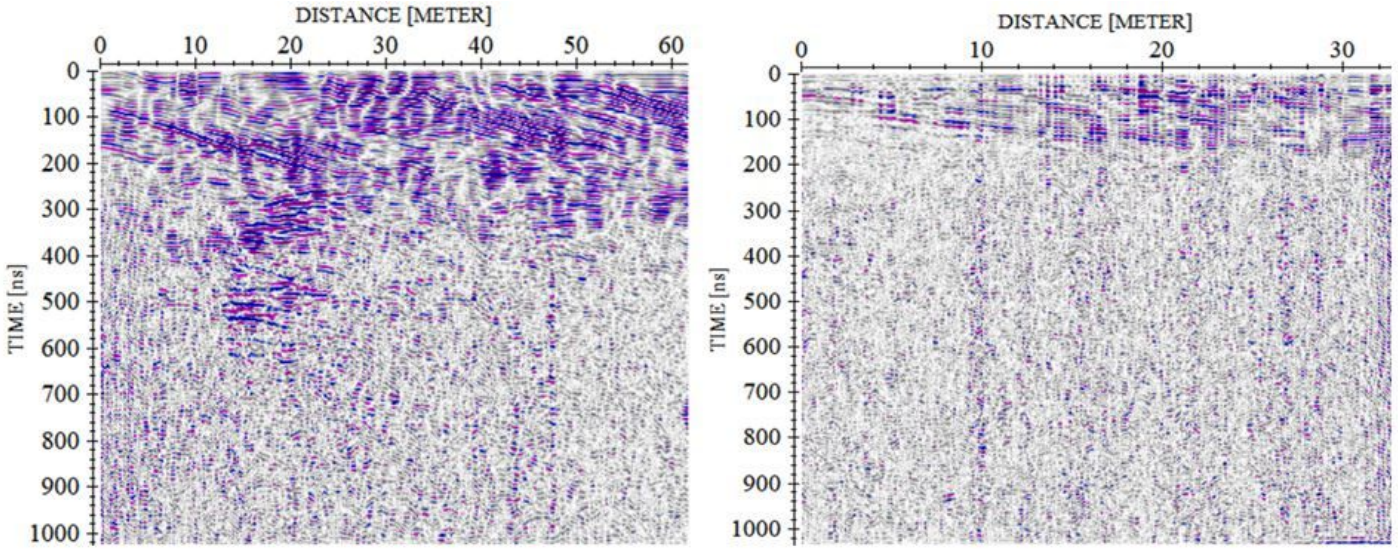

(a) (b)

Figure 9

GPR images of the site-1 (a) and site-2 (b). Some tilt signals coming from the reflection of tree trunks and roots may mix with the other tilt signals from the subsurface inclined interfaces.

Figure 10

Photograph of detecting paddy land. The surface soil moisture content is 31.8% by measurements in situ.

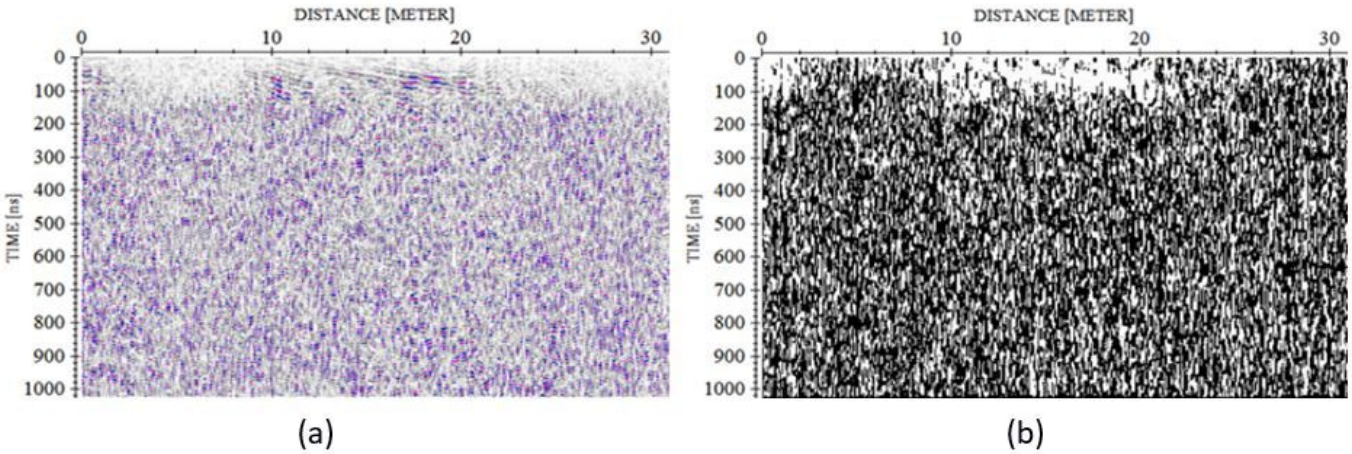

Figure 11

GPR data of the paddy land (a) and its coherence attribute (b), the black color is low value and the white is high in the coherence image

Figure 12

Photograph shows GPR acquisition on grass land soil under high voltage lines

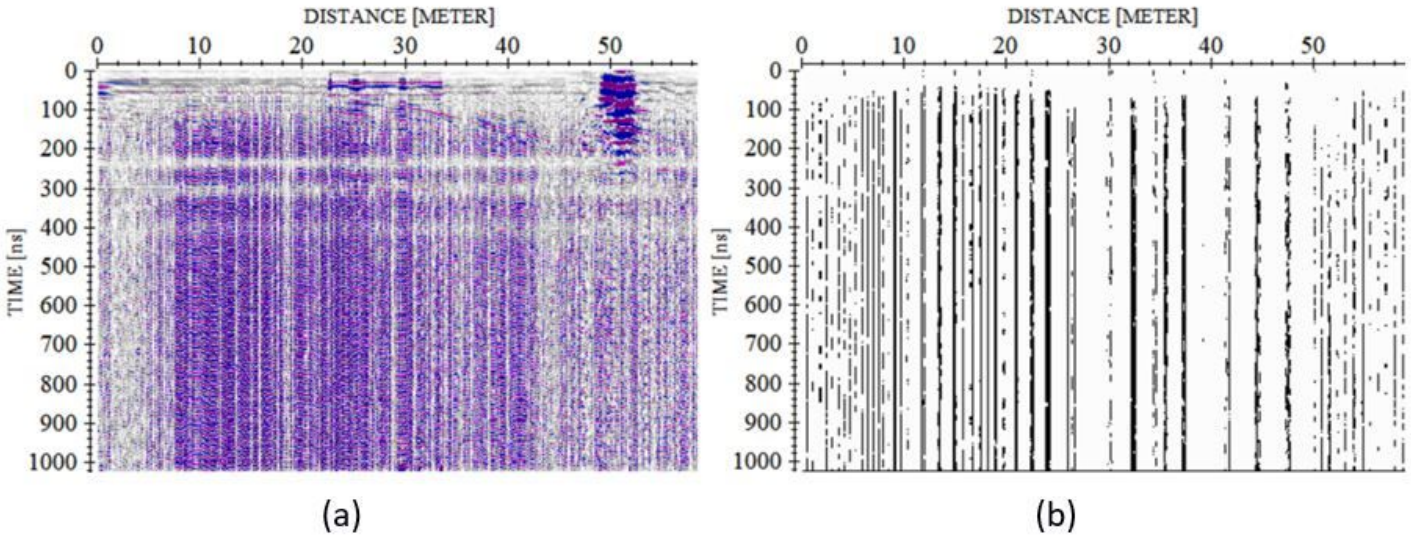

Figure 13

Conventional GPR image (a) and its coherence attribute (b)

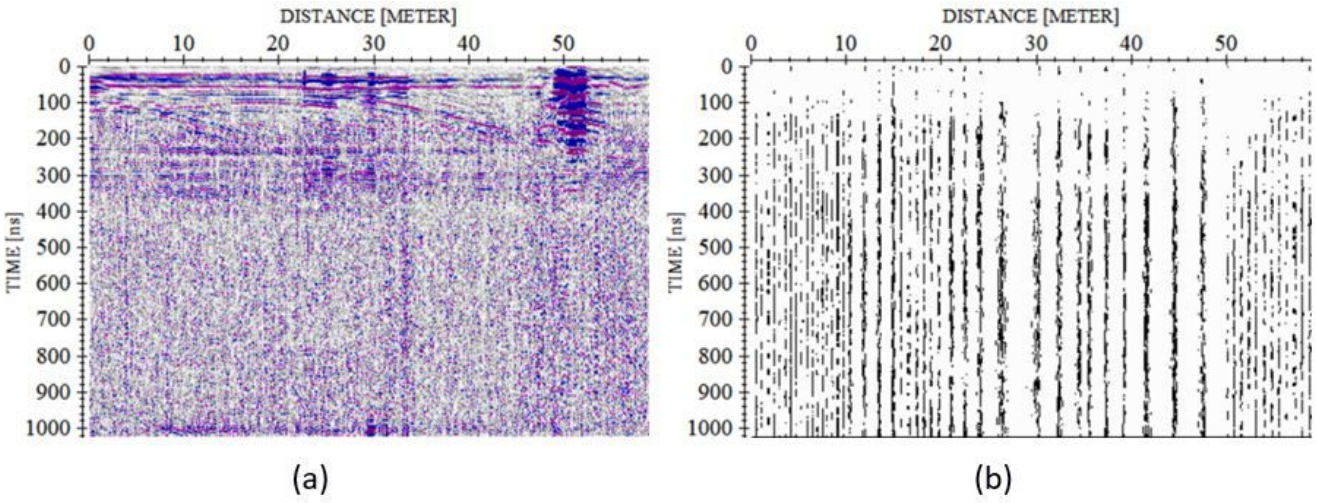

Figure 14

GPR data processed by F-K filtering (a) and its coherence attribute (b)

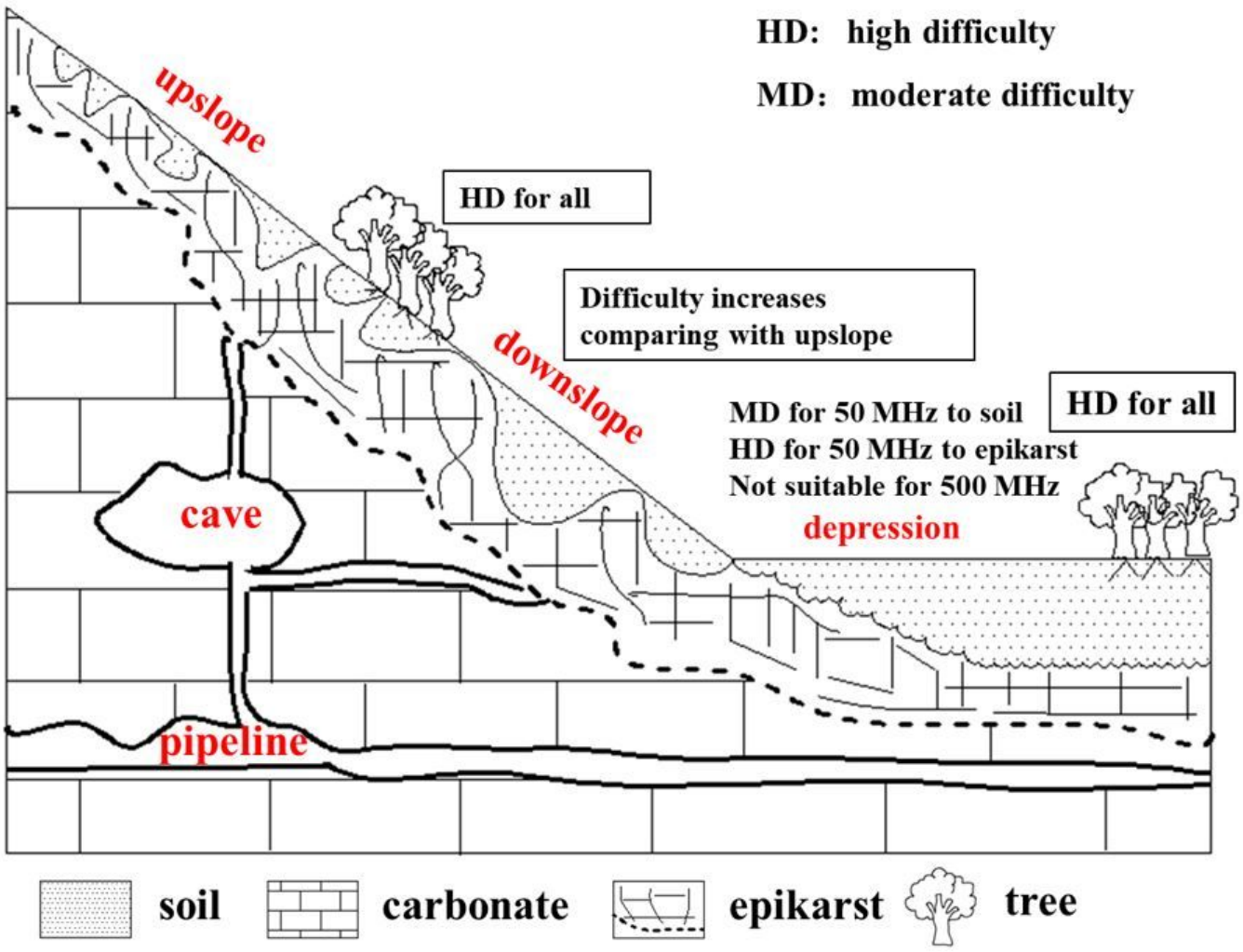

Figure 15

The conceptual diagram explaining different aspects of GPR potential evaluation in peak-cluster depression study.

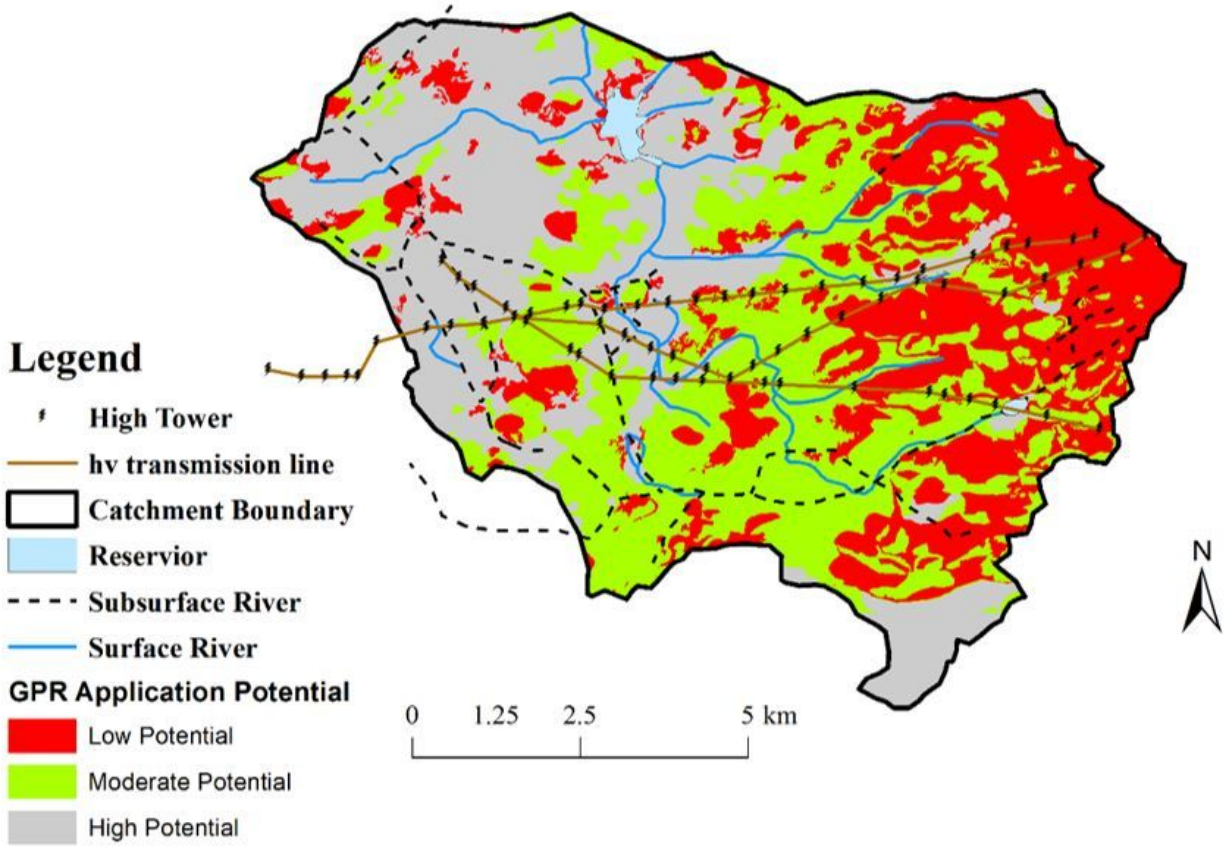

Figure 16

GPR application potential categorization for the Houzhai catchment

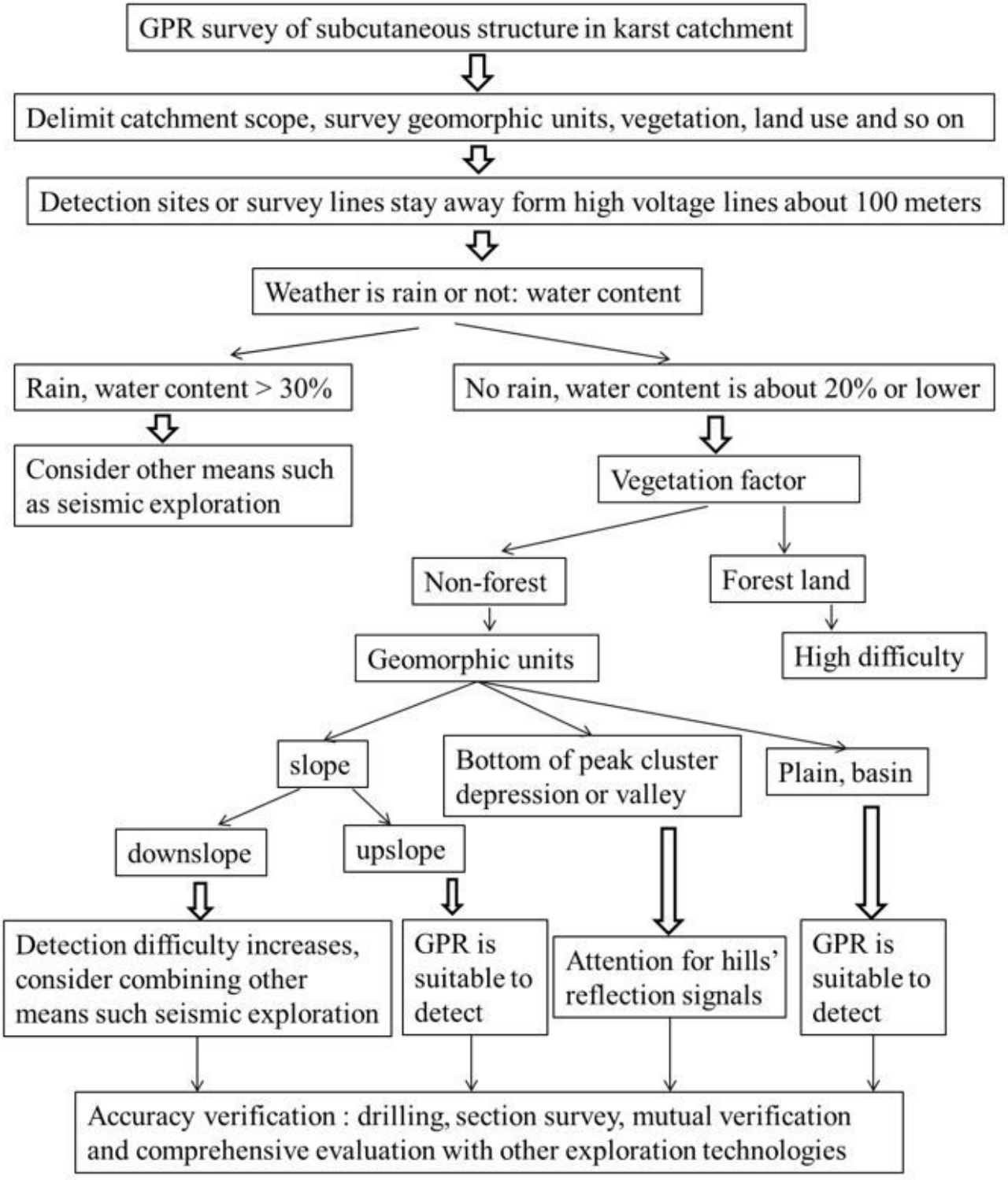

Figure 17

Application paradigm of GPR to shallow surface structure survey in karst catchment